nature photonics

SUPPLEMENTARY INFORMATION

DOI: 10.1038/NPHOTON.2015.21

Subwavelength anti-diffracting beams propagating over more than 1,000 Rayleigh lengths

E. DelRe,[1] F. Di Mei,[1,2] J. Parravicini,[1] GB. Parravicini,[3] A. J. Agranat,[4] and C. Conti[5]

[1]*Physics Department, University of Rome Sapienza, 00185 Rome, Italy*
[2]*Center for Life Nano Science@Sapienza, Istituto Italiano di Tecnologia, 00161 Rome, Italy*
[3]*Physics Department, University of Pavia, 27100 Pavia, Italy*
[4]*Applied Physics Department, Hebrew University of Jerusalem, 91904 Israel*
[5]*Institute for Complex Systems, National Research Council (ISC-CNR), Via dei Taurini 19, 00185 Rome, Italy**

(Dated: January 9, 2015)

SUPPLEMENTARY INFORMATION

Beam anti-diffraction law in the paraxial KGE regime

The starting model for the optical amplitude A in the paraxial approximation, is written as

$$2ik\frac{\partial A}{\partial z}+\nabla_{\perp}^{2}A-\frac{L^{2}}{\lambda^{2}}\left(\frac{\nabla_{\perp}|A|^{2}}{2|A|^{2}}\right)^{2}A=0. \qquad (1)$$

Separating the variables,

$$A(x,y,z)=\alpha(x,z)\beta(y,z), \qquad (2)$$

α obeys the equation

$$2ik\frac{\partial\alpha}{\partial z}+\frac{\partial^{2}\alpha}{\partial x^{2}}-\frac{L^{2}}{\lambda^{2}}\frac{\left(\partial_{x}|\alpha|^{2}\right)^{2}}{4|\alpha|^{4}}\alpha=0, \qquad (3)$$

while the same equation applies for β with x replaced by y. Eq. (3) is satisfied by (α_0 is an arbitrary constant)

$$\alpha(x,z)=\frac{\alpha_{0}}{\sqrt{w_{x}(z)}}e^{-\frac{x^{2}}{w_{x}^{2}(z)}+i\left[\phi_{0}(z)+\frac{1}{2}\phi_{2}(z)x^{2}\right]} \qquad (4)$$

with

$$\phi_{0}(z)=-\frac{1}{kw_{0x}^{2}}\frac{\tan^{-1}(\sqrt{a}z)}{\sqrt{a}} \qquad (5)$$

and

$$\phi_{2}(z)=\frac{az}{1+az^{2}}, \qquad (6)$$

with $a\equiv(1-L^{2}/\lambda^{2})/k^{2}w_{0x}^{4}$; w_{ox} is the arbitrary initial beam in the $x-$direction. The waist of the beam in the $x-$direction (analogous for the $y-$direction) along the propagation direction z is

$$w_{x}(z)=w_{0x}\sqrt{1+\frac{4}{k^{2}w_{0x}^{4}}\left[1-\left(\frac{L^{2}}{\lambda^{2}}\right)\right]z^{2}}. \qquad (7)$$

For an initially radially symmetric beam, such that $w_{ox}=w_{oy}=w_0$, the circular waist in two transverse dimensions is given by

$$w(z)=w_{0}\sqrt{1+\frac{4}{k^{2}w_{0}^{4}}\left[1-\left(\frac{L^{2}}{\lambda^{2}}\right)\right]z^{2}}, \qquad (8)$$

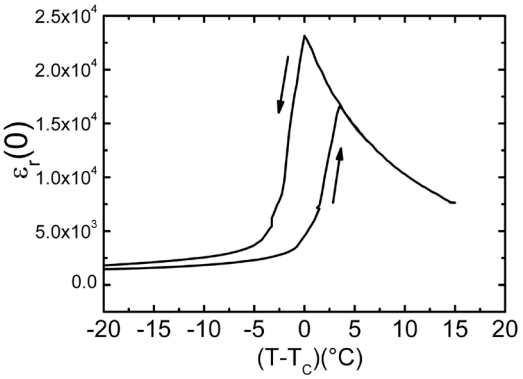

FIG. 1: (Figure S1.) Thermal hysteresis in the low-frequency relative dielectric constant $\epsilon_r(0)$. The macroscopic difference between the cooling and heating curves signals the presence of a non-ergodic behavior in proximity of the Curie point.

which, for the paraxial condition $kw_0\gg1$, gives Eq.(1) of the main text. The effect is expected for all wavelengths for which photorefractive response is efficient (400-800 nm). For $\lambda_1\neq\lambda_2$,$L_1\neq L_2$ because n_0 depends on λ_i, so that propagation will be described by $L_1/\lambda_1\neq L_2/\lambda_2$, and anti-diffraction will intervene at λ_i when $L_i/\lambda_i>1$.

Identification of the non-ergodic region near T_C

In Fig.(S1) we report dielectric constant measurements on the sample. The electric field is delivered through plane parallel electrodes sputtered on the crystal facets using a precision LCR-meter (Agilent- 4284A) applying a 100 mV voltage at the frequency of 1 kHz. Temperature variations are achieved through a closed two stage helium cryostat (in a vacuum configuration) for the range 250-300 K, with a scan rate of 0.1 K/min. The acquisition time of 5 ms and the slow T scan rate render each single $\epsilon_r(0)$ measurement isothermal. Temperature is monitored through a calibrated silicon diode. The strong thermal hysteresis (i.e., dependence of the $\epsilon_r(0)$ versus

DOI: 10.1038/NPHOTON.2015.21

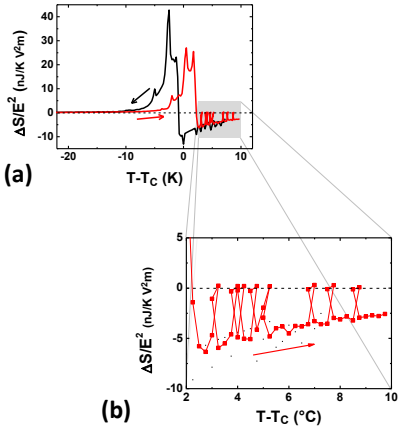

FIG. 2: (Figure S2.) (a) Dielectric measurements of the Fröhlich entropy [3–5] (per volume unit, normalized to the squared probe-field amplitude) in proximity of the Curie point and (b) blow-up of shaded region illustrating phase-fluctuations from liquid-like to solid in the heating stage.

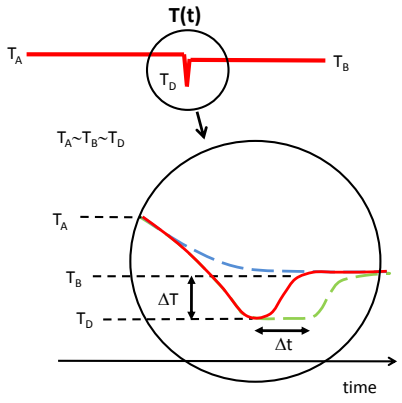

FIG. 3: (Figure S3.) **Quasi-isothermal preparation protocol based on a non-monotonic** $T(t)$**.** Temperature shocks versus standard cooling. Schematic of the thermal shock associated to the quasi-isothermal excitation of an out-of-equilibrium response along with details of the shock, i.e., depth of the shock ΔT and duration of the shock Δt (note the three examples)

T curve on the fact that cooling or heating is being enacted) that emerges in proximity of the temperature at which the $\epsilon_r(0)$ peaks (T_C) pinpoints the cross-over region, i.e., where the crystal response is history-dependent (non-ergodic). To analyze in more detail the nature of the non-ergodic phase, in Fig.(S2) we report the changes of entropy (for unit volume) in isothermal conditions in response to the application of the probing alternating bias field of amplitude E [1–5]

$$S(T) = S_0(T) + \frac{E^2\epsilon_0}{2}\frac{\partial\epsilon_r(0)}{\partial T} = S_0(T) + S_E(T), \quad (9)$$

where S_0 is the entropy of the system at zero field, ϵ_0 is the vacuum permittivity, $\epsilon_r(0)$ is the quasi-static relative dielectric constant (associated to the real part of the dielectric susceptibility in the low frequency limit), and T is the absolute temperature of the crystal. Specifically, S_E is the entropy change associated to the polarization of the dielectric in response to the field, and is proportional to $\partial\epsilon_r(0)/\partial T$: the application of an electric field increases the entropy if $\partial\epsilon_r(0)/\partial T$ is positive, while it decreases entropy if the same quantity is negative. In disordered systems, e.g. in liquids, an applied field creates order, since it orients the electric dipoles (permanent or field-induced) otherwise randomly arranged. As a consequence, the entropy variation induced by the field is negative, then $\partial\epsilon_r(0)/\partial T$ is negative. On the contrary, in crystalline solids under an electric field, a fraction of the dipoles undergoes discontinuous transitions between preferred orientations: this gives rise to an increase of the entropy of the system, then $\partial\epsilon_r(0)/\partial T$ is positive. When phase transitions are considered, a solid-solid (order/order) transition manifests itself as a variation of the positive slope of the $\epsilon_r(0)$ versus T curve, since the entropy contribution supplied by the field is positive both before and after the transition, with values in accordance to the degree of order of the two phases. In turn, a solid-liquid (order/disorder) transition will amount to a slope reversal and in S_E as a change from positive to negative values. The rapid and erratic shifts from the low to the high entropy states reported in Fig.(S2) indicate a dynamic phase for $T - T_C > 3°\text{C}$.

Naturally converging beams in the $\epsilon_\text{m} < 0$ regime

The $\epsilon_\text{m} < 0$ regime profoundly alters the effects of diffraction. In a standard material with $\epsilon > 0$, point-like sources give rise to spherical waves: to achieve a point-like focus, we need to converge light from all possible directions and, equally, to observe a point-like detail, we need to collect light from all angles. In practice, only a part of this ideal sphere is accessible, so that the achievable resolution is much less than that conceptually compatible with propagation theory, $w_0 \sim \lambda/2n$, where w_0

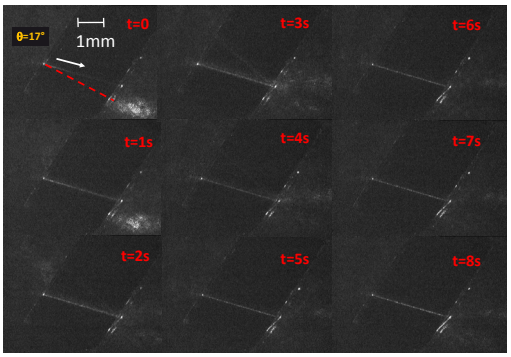

FIG. 4: (Figure S4.) **Time evolution of anti-diffraction.** Time sequence of the HE-KGE transition for the propagating beams showing how the shrinking beam regime is time resolved.

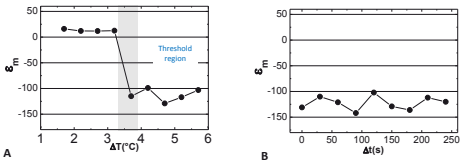

FIG. 5: (Figure S5.) (a) Values of minimum $\epsilon_{\rm m}$ as a function of the amplitude ΔT identifies the existence of a threshold region that activates the dipolar glass in the equilibrated state at the operating temperature T_B, as expected for a glassy system subject to nonmonotonic thermal trajectories. (b) Independence of the minimum value of $\epsilon_{\rm m}$ for an above-threshold $\Delta T(t) = 4.7°$C on the dwell time Δt at the lower quenching T_D of the trajectory.

is the minimum spot size, λ the optical wavelength, and n the material index of refraction. w_0 and the angular portion of the wave-vectors intercepted Δk_0 form a trade-off governed by the inequality $(\Delta k_0)^2 w_0^2 > 1/n^2 = 1/\epsilon_r$, where $k_0 = 2\pi/\lambda$ is the vacuum optical wave-number, ϵ_r the relative material permittivity at optical frequencies. This trade-off limits all optical systems. For example, for paraxial beams, in the focal plane of a lens of focal length f the beam spot is at minimum $w_0 \simeq f\lambda/w\pi n$, where w is the spot of the input beam. This implies that to observe small micrometric details optically, large objectives with short focal lengths are required, and this limits our ability to observe objects embedded deep in a sample. In the $\epsilon < 0$ case, the relative sign of the transverse diffraction operator changes in the paraxial propagation equation, and the trade-off condition poses no limitations. In this case, beams can be made to converge irrespective of the intercepted angular spread. The $\epsilon < 0$ regime overcomes the limits associated to the trade-off inequality and enhances spatial resolution in a manner analogous to a perfect lens in metamaterials, but without the requirement of a nearby optical resonance and a simultaneous $\mu < 0$ response. We underline that close enough to the point-like focus z_c, light will be transferred into the realm of non-paraxial optics, typical of subwavelength propagation.

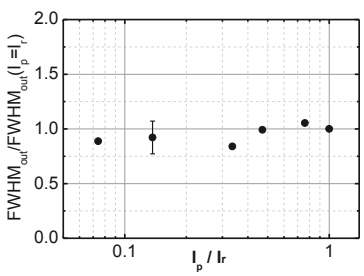

* eugenio.delre@uniroma1.it

[1] Parravicini, G.B., Stella, A., Tognini, P., Merli, P.G., Migliori, A., Cheyssac, P., Kofman, R. Insight into the premelting and melting processes of metal nanoparticles through capacitance measurements. *Appl. Phys. Lett.* **82**, 1461-1463 (2003).

[2] Sassella, A., Braga, D., Campione, M., Ciabattoni, T., Moret, M., Parravicini, J., and Parravicini, G.B. Probing phase transitions and stability of organic semiconductor single crystals by dielectric investigation. *J. Appl. Phys.* , **109**, 013529 (2011)

[3] Parravicini, G. B., Campione, M., Marabelli, F., Moret, M., Sassella, A. Experimental assessment of nonergodicity in tetracene single crystals. *Phys. Rev. B* **86**, 024107 (2012).

[4] Fröhlich, H. *Theory of Dielectrics* (Clarendon Press, 1957).

[5] Scaife, B.K. *Principles of Dielectrics* (Clarendon Press, 1998).

DOI: 10.1038/NPHOTON.2015.21

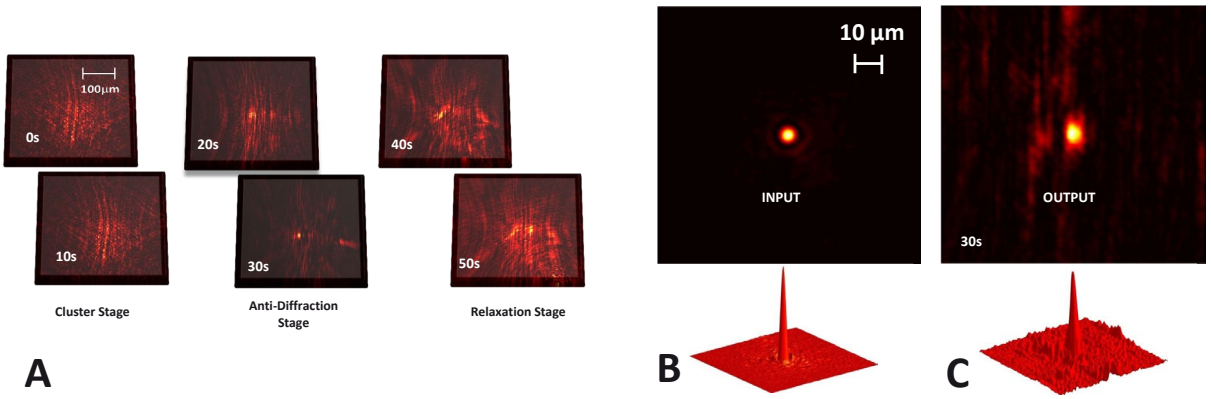

FIG. 7: (Figure S7.) **Precursor phenomena in the formation of ultra-tight beams.** The crystal is initially rapidly cooled (at a cooling rate of 0.08 °C/s) to the lower quenching temperature $T_D = 10$°C. In distinction to previous thermal shock experiments, the crystal is at this point exposed to the propagating beam. It is then reheated to $T_B = 14.5$°C, the final operating temperature, at a heating rate of 0.2 °C/s. (a) Wide area (low resolution) images of the intensity distribution. Initially the beam encounters a locked , cluster-like, structure reminiscent of the ferroelectric state that subsequently gives way to a disordered structure where clustering is absent. As this occurs, the beam collapses from a highly disordered output intensity distribution to a localized spot, to then subsequently relax into a once again disordered and scattered output distribution. (b) Input intensity distribution and three-dimensional rendering. (c) Output intensity distribution and three-dimensional rendering after 30s from the instant in which T_D is reached.